nature immunology

SUPPLEMENTARY INFORMATION

https://doi.org/10.1038/s41590-019-0441-y

In the format provided by the authors and unedited.

PD-1 blockade in subprimed CD8 cells induces dysfunctional PD-1^{+}CD38^{hi} cells and anti-PD-1 resistance

Vivek Verma[1,11], Rajeev K Shrimali[1,12], Shamim Ahmad[1,13], Winjie Dai[1], Hua Wang[1], Sumin Lu[1], Rahul Nandre[1,11], Pankaj Gaur[1,11], Jose Lopez[11], Moshe Sade-Feldman[2,3], Keren Yizhak[3], Stacey L. Bjorgaard[2,3], Keith T. Flaherty[2], Jennifer A. Wargo[4], Genevieve M. Boland[5], Ryan J. Sullivan[2], Gad Getz[2,3,6], Scott A. Hammond[7], Ming Tan[8], Jingjing Qi[9], Phillip Wong[9], Taha Merghoub[9,10], Jedd Wolchok[9,10], Nir Hacohen[2,3], John E. Janik[1,14], Mikayel Mkrtichyan[1,11,15], Seema Gupta[1,11] and Samir N. Khleif[1,11]*

[1]Georgia Cancer Center, Augusta University, Augusta, GA, USA. [2]Department of Medicine, Massachusetts General Hospital Cancer Center, Boston, MA, USA. [3]Broad Institute of Massachusetts Institute of Technology and Harvard, Cambridge, MA, USA. [4]Department of Surgical Oncology, University of Texas MD Anderson Cancer Center, Houston, TX, USA. [5]Department of Surgery, Massachusetts General Hospital, Boston, MA, USA. [6]Department of Pathology, Massachusetts General Hospital, Boston, MA, USA. [7]MedImmune LLC, Gaithersburg, MD, USA. [8]Department of Biostatistics, Bioinformatics & Biomathematics, Georgetown University, Washington, DC, USA. [9]Memorial Sloan Kettering Cancer Center, New York, NY, USA. [10]Weill Cornell Medical and Graduate Schools, New York, NY, USA. [11]Present address: The Loop Immuno-Oncology Laboratory, Lombardi Comprehensive Cancer Center, Georgetown University Medical Center, Washington, DC, USA. [12]Present address: Therapeutic Discovery, MD Anderson Cancer Center, Houston, TX, USA. [13]Present address: Five Prime Therapeutics Inc., South San Francisco, CA, USA. [14]Present address: Incyte Inc., Wilmington, DE, USA. [15]Present address: A2 Biotherapeutics, Agoura Hills, CA, USA. *e-mail: snk48@georgetown.edu

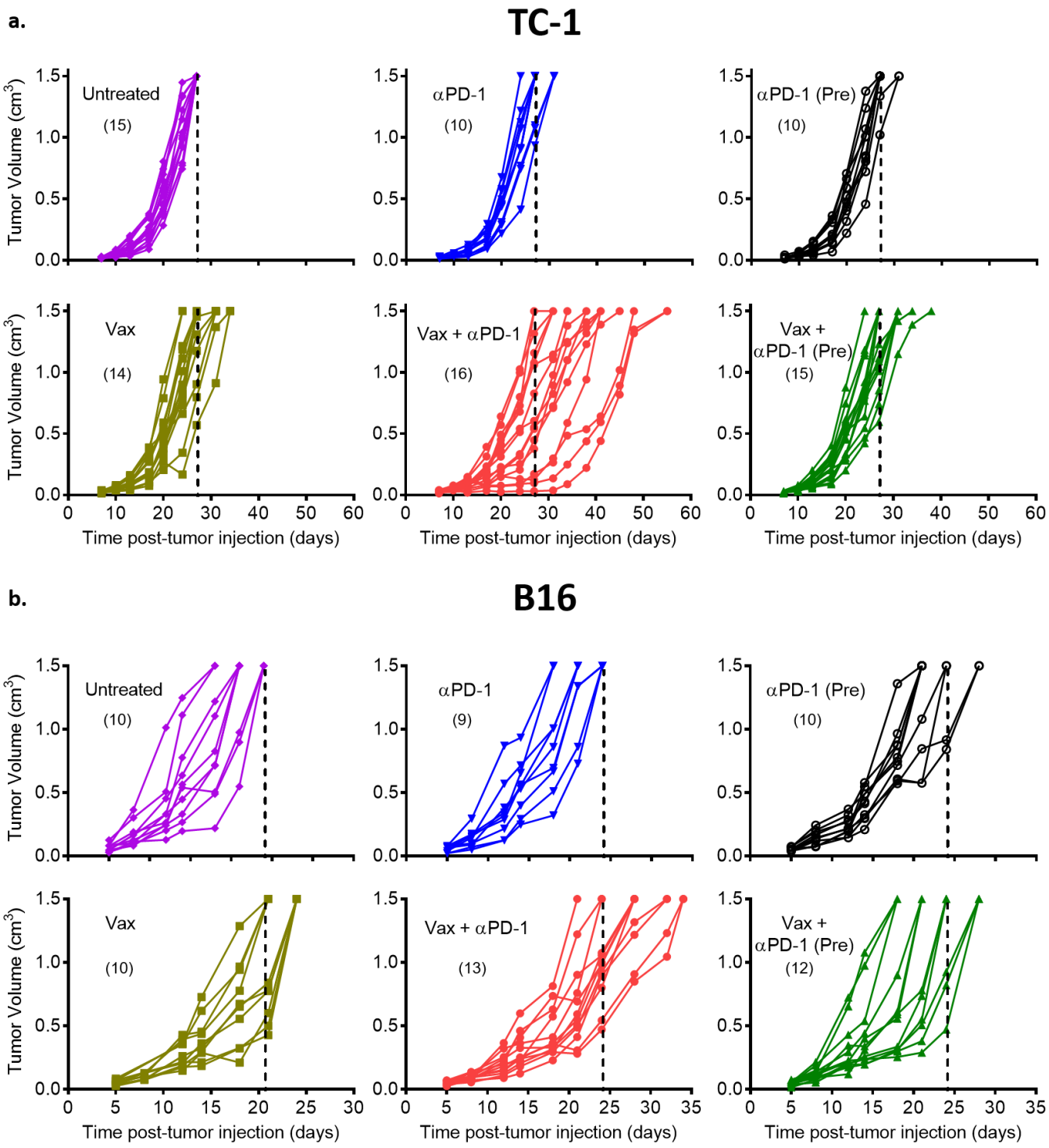

Supplementary Figure 1

Anti-PD-1 prior to antigenic stimulation abrogates the anti-tumor effects of Vax + αPD-1.

Tumor growth profiles of individual mice after various treatments in TC-1 (**a**) and B16 (**b**) tumor models. Experiments were repeated twice with an indicated number of mice/group.

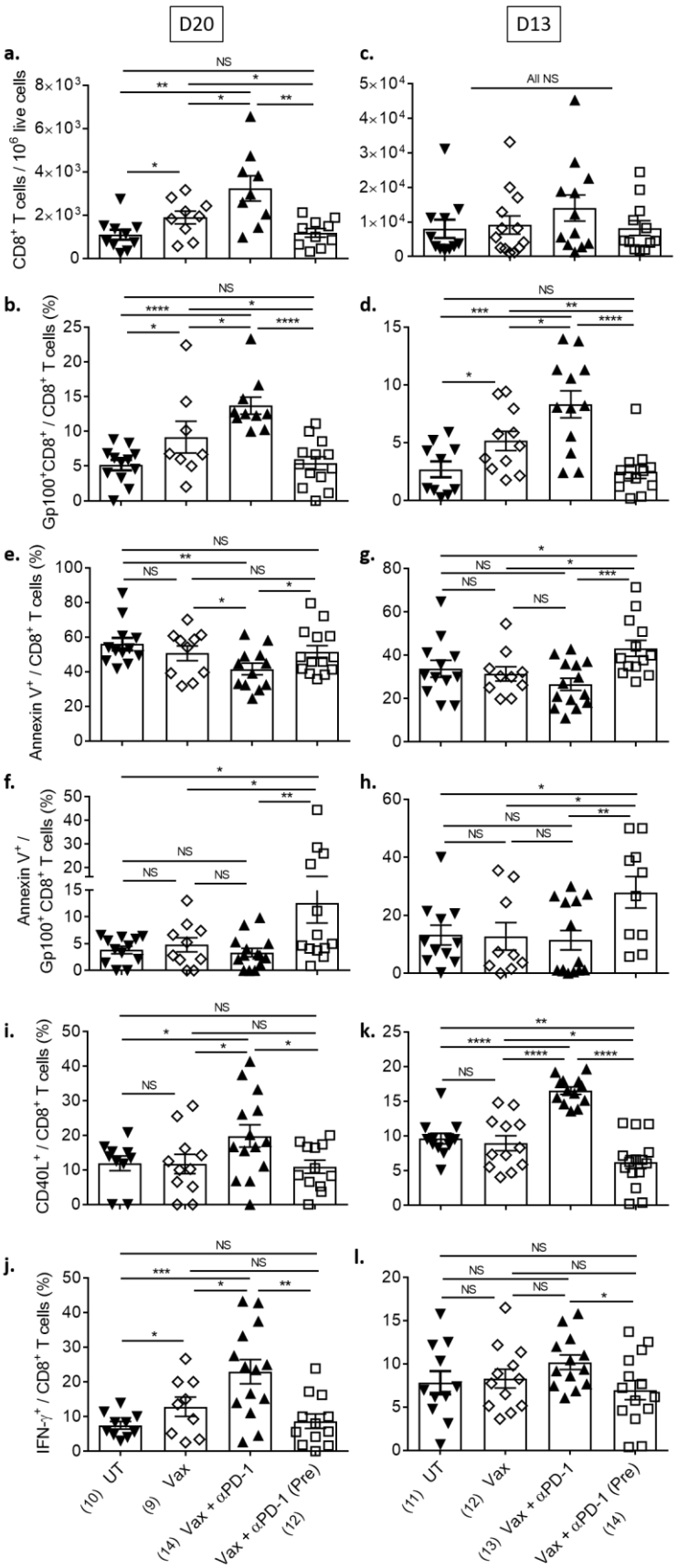
D20
D13
a.
c.
b.
d.
e.
g.
f.
h.
i.
k.
j.
l.
CD8+ T cells / 10^6 live cells
Gp100+CD8+ / CD8+ T cells (%)
Annexin V+ / CD8+ T cells (%)
Annexin V+ / Gp100+ CD8+ T cells (%)
CD40L+ / CD8+ T cells (%)
IFN-γ+ / CD8+ T cells (%)
All NS
NS
(10) UT
(9) Vax
(14) Vax + αPD-1
Vax + αPD-1 (Pre) (12)
(11) UT
(12) Vax
(13) Vax + αPD-1
Vax + αPD-1 (Pre) (14)

Supplementary Figure 2

Prior PD-1 blockade abrogates vaccine-induced tumor-specific immune responses early during the course of treatment**.**

Tumor tissues were harvested 3 days after priming (D13) or three days after boosting (D20) from B16 melanoma-bearing mice. **a-d**. Numbers of total (**a** & **c**) and antigen-specific $CD8^+$ T cells (**b** & **d**) at D20 (**a-b**) and at D13 (**c-d**). **e-h**. Frequencies of Annexin V^+ total (**e** & **g**) and antigen-specific $CD8^+$ T cells (**f** & **h**) in the TME at D20 (**e-f**) and at D13 (**g-h**) as indicated. **i-l**. Frequencies of $CD40L^+$ (**i** and **k**) and IFN-γ^+ (**j** & **l**) $CD8^+$ T cells in the TME at D20 (**i-j**) and at D13 (**k-l**) as indicated. Flow cytometry data are the average of two independent experiments. Each dot corresponds to one mouse with the indicated number of mice per group given in parentheses. For comparison purposes, an unpaired, one-tailed Student's *t*-test was used. The error bars indicate the s.e.m. ^{NS}non-significant (**a**) *(lower) p=0.0228, *(middle) p=0.0277, *(upper) p=0.0286, **(left) p=0.0012, **(right) p=0.0014; (**b**) *(lower) p=0.0333, *(middle) p=0.042, *(upper) p=0.0472, $^{****}p\leq0.0001$; (**d**) *(lower) p=0.018, *(upper) p=0.0207, $^{**}p$=0.0072, $^{***}p$=0.0004, $^{****}p\leq0.0001$; (**e**) *(lower) p=0.05, *(upper) p=0.03, $^{**}p$=0.0041; (**f**) *(lower) p=0.0462, *(upper) p=0.0181, $^{**}p$=0.0094; (**g**) *(lower) p=0.0157, *(upper) p=0.0469, $^{***}p$=0.0006; (**h**) *(lower) p=0.0265, *(upper) p=0.0152, $^{**}p$=0.0062 (**i**) *(left) p=0.0384, *(middle) p=0.0399, *(right) p=0.0165; (**j**) *(lower) p=0.0414, *(upper) p=0.0260, $^{**}p$=0.0013, $^{***}p$=0.0007; (**k**) $^{*}p$=0.0343, $^{**}p$=0.006, $^{****}p\leq0.0001$; (**l**) $^{*}p$=0.0156. $^{*}P \leq 0.05$; $^{**}P \leq 0.01$; $^{***}P \leq 0.001$; $^{****}P \leq 0.0001$.

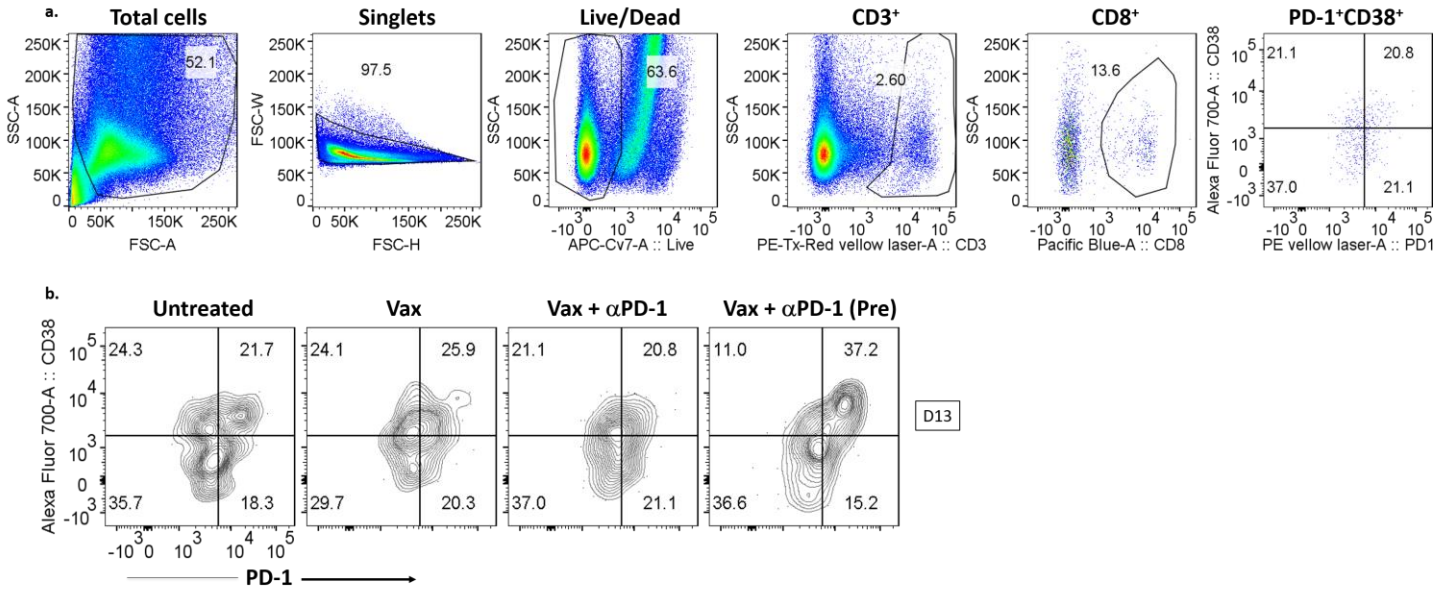

Supplementary Figure 3

PD-1 blockade prior to antigenic stimulation generates dysfunctional PD-1^{+}CD38^{+} CD8^{+} T cells.

a. Gating strategy. **b**. FACS contour plots showing frequency of PD-1^{+}CD38^{+} cells in total CD8^{+} T cells in the tumors (at D13) following various treatments.

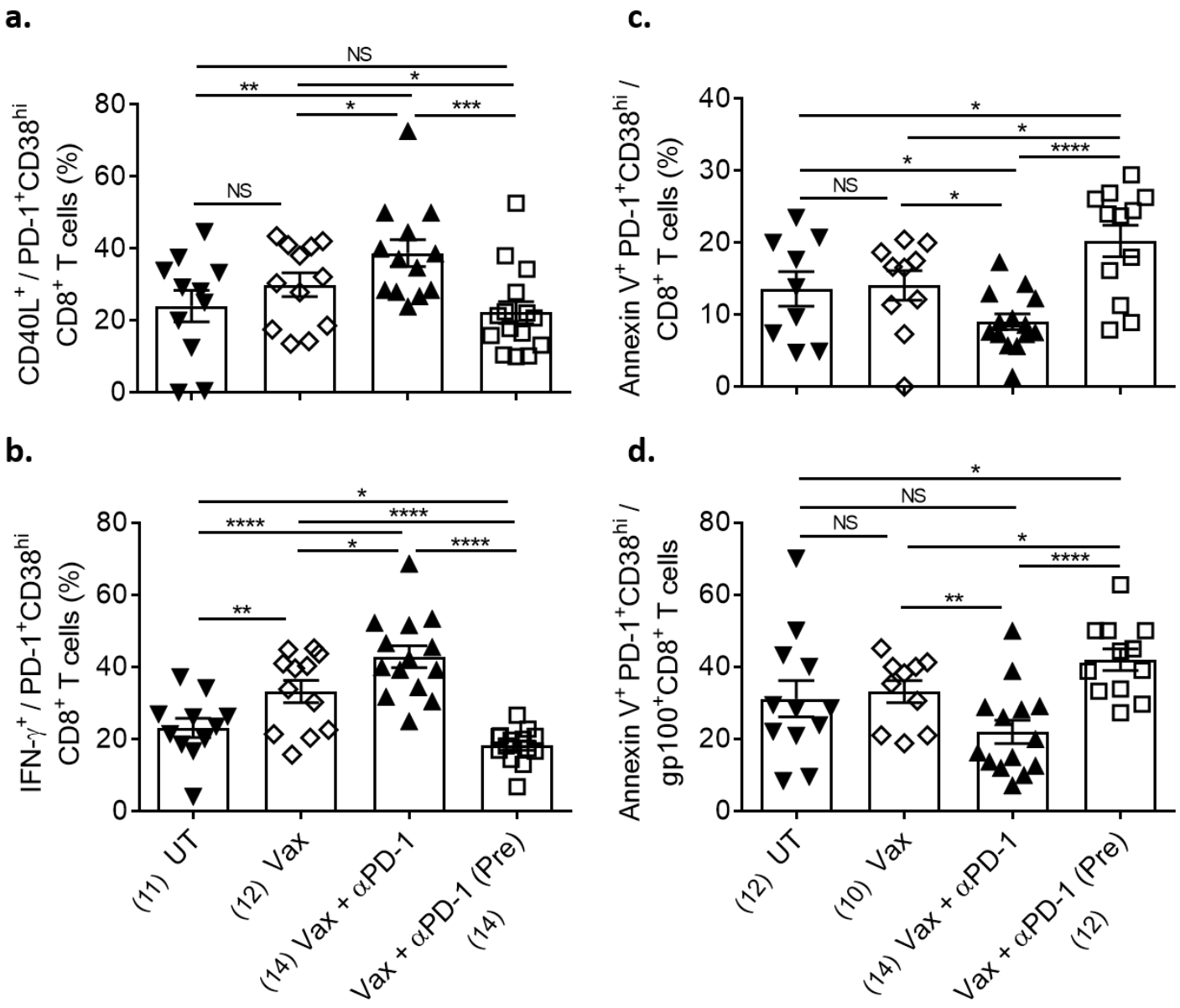

Supplementary Figure 4

PD-1^{+}CD38^{hi} CD8^{+} T cells induced as a result of anti-PD-1 pre-treatment are dysfunctional.

a-b. Frequency of CD40L^{+} (**a**) and IFN-γ^{+} (**b**) T cells in PD-1^{+}CD38^{hi} CD8^{+} T cell population. **c-d.** Frequencies of Annexin V^{+} PD-1^{+}CD38^{hi} cells in total (**c**) and antigen-specific (**d**) CD8^{+} T cells at D13 post-B16 tumor implantation. Data are the average of two independent experiments. Each dot corresponds to one mouse with the indicated number of mice per group given in parentheses. The error bars indicate the s.e.m. For comparison purposes, an unpaired, one-tailed Student's *t*-test was used. ^{NS}non-significant (**a**) *(lower) p=0.0463, *(upper) p=0.0496, $^{**}p$=0.0086, $^{***}p$=0.0009; (**b**) *(lower) p=0.018, *(upper) p=0.0441, $^{**}p$=0.01, $^{****}p\leq0.0001$; (**c**) vs. UT: *(lower) p=0.0327 and *(upper) p=0.0275, vs. Vax: *(lower) p=0.0143 and *(upper) p=0.0273, $^{****}p\leq0.0001$; (**d**) *(lower) p=0.026, *(upper) p=0.0382, $^{**}p$=0.01, $^{****}p\leq0.0001$. $^{*}P \leq 0.05$; $^{**}P \leq 0.01$; $^{***}P \leq 0.001$; $^{****}P \leq 0.0001$.

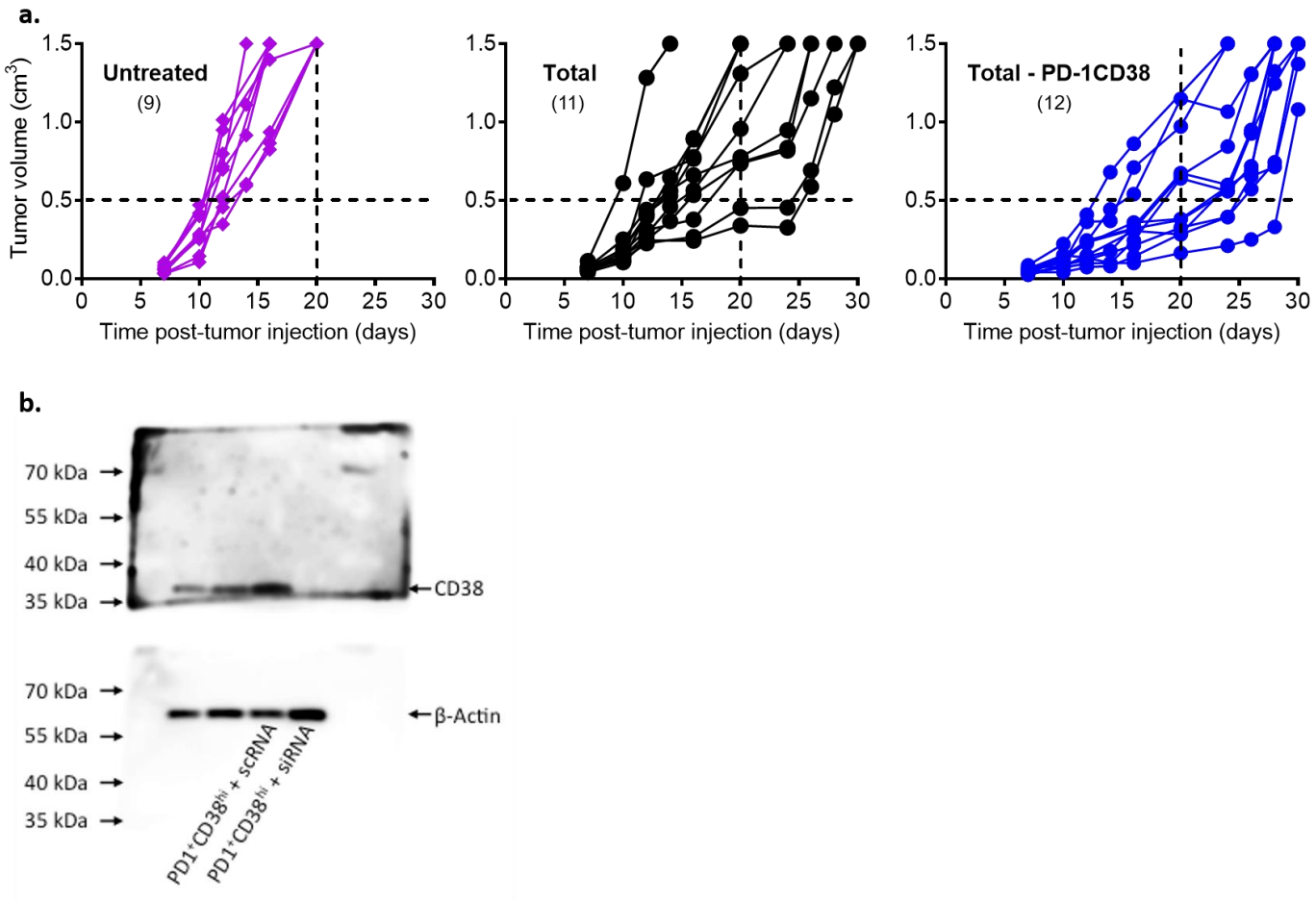

Supplementary Figure 5

Depletion of PD-1^{+}CD38^{hi} CD8^{+} T cells results in strong anti-tumor response.

a. Tumor growth of variously treated B16-bearing *Rag1*$^{-/-}$ mice following transfer of either total or PD-1^{+}CD38^{+} depleted, *in vitro* activated CD8^{+} T cells (with an indicated number of mice per group given in parentheses). **b.** The full scan of the blot showing the expression of CD38 and β-actin in flow-sorted PD-1^{+}CD38^{+} T cells transfected either with scrambled RNA (scRNA) or CD38 siRNA.

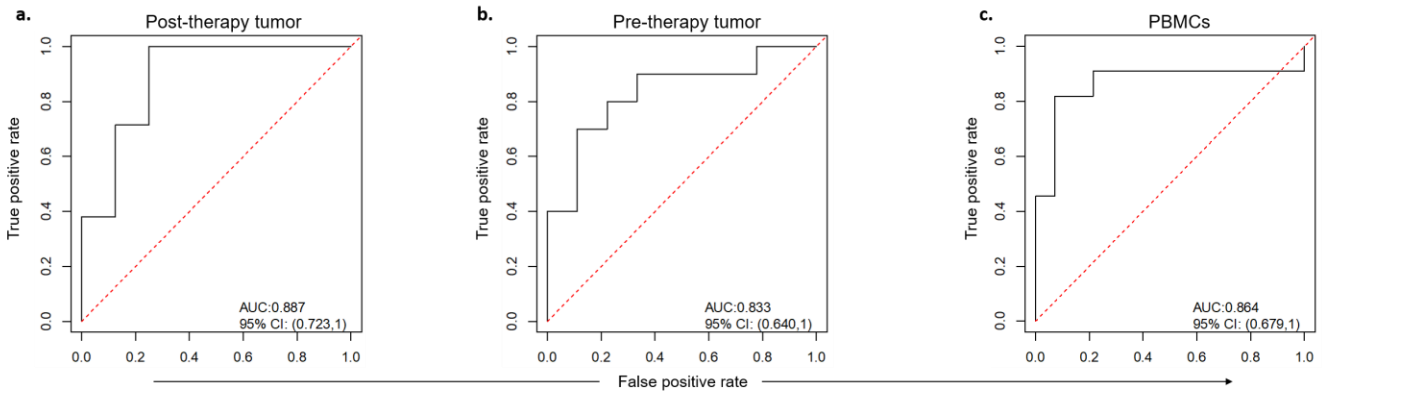

Diagnostic table when cut-off is 4%#

		True	
		Disease/NR	Non-disease/R
Experiment	Disease/NR	21	2
	Non Disease/R	0	6

$$\text{Sensitivity} = \frac{TP}{TP + FN} = 1.000$$
$$\text{Specificity} = \frac{TN}{TN + FP} = 0.75$$
$$\text{PPV} = \frac{TP}{TP + FP} = 0.913$$
$$\text{NPV} = \frac{TN}{TN + FN} = 1.000$$

Diagnostic table when cut-off is 10%^

		True	
		Disease/NR	Non-disease/R
Experiment	Disease/NR	8	3
	Non Disease/R	2	6

$$\text{Sensitivity} = \frac{TP}{TP + FN} = 0.800$$
$$\text{Specificity} = \frac{TN}{TN + FP} = 0.667$$
$$\text{PPV} = \frac{TP}{TP + FP} = 0.727$$
$$\text{NPV} = \frac{TN}{TN + FN} = 0.75$$

Diagnostic table when cut-off is 5%*

		True	
		Disease/NR	Non-disease/R
Experiment	Disease/NR	9	1
	Non Disease/R	2	13

$$\text{Sensitivity} = \frac{TP}{TP + FN} = 0.818$$
$$\text{Specificity} = \frac{TN}{TN + FP} = 0.929$$
$$\text{PPV} = \frac{TP}{TP + FP} = 0.900$$
$$\text{NPV} = \frac{TN}{TN + FN} = 0.867$$

Supplementary Figure 6

ROC analysis to measure the predictive power of $CD38^+$ fraction of $PD1^+CD8^+$ T-cells pre- and post- anti-PD-1 therapy in the human tumor and PBMC samples.

a-c. The ROC curves were generated using R version 3.5.1 software in post-therapy tumors with 4% cut-off (**a**), pre-therapy tumors with 10% cut-off (**b**), and PBMCs with 5% cut-off (**c**). AUC and 95% confidence interval (CI) were determined using Delong method with R version 3.5.1 statistical software. The diagnostic tables used for generating each ROC curve as well as the formulae used to calculate sensitivity, specificity, PPV and NPV are provided.

Comparison of responding vs. non-responding tumor lesions that had more than 4%$^{\#}$ or 10%$^{\wedge}$ $PD\text{-}1^+CD38^+$ cells in the $CD8^+$ population in the TME. *For human PBMC data, the $CD38^+$ fraction of $PD\text{-}1^+CD8^+$ T cells that showed more than 5% decline at 9 weeks when compared with 3 weeks were compared between responders and non-responders post-therapy. AUC: Area Under the Receiver Operating Characteristics (ROC) Curve; AUC 95% CI: There is 95% of confidence that the interval contains the true AUC. For example, there is 95% confidence that (0.679,1) contains the true value of AUC for 5% cut-off; PPP: Positive predictive value; NPV: Negative predictive value.